Mixed convection and stability analysis of stagnation-point boundary layer flow and heat transfer of hybrid nanofluids over a vertical plate

Received 22 August 2019
Revised 6 October 2019
Accepted 10 October 2019

Mohammad Ghalambaz
Department for Management of Science and Technology Development, Ton Duc Thang University, Ho Chi Minh City, Vietnam and Faculty of Applied Sciences, Ton Duc Thang University, Ho Chi Minh City, Vietnam

Natalia C. Roşca
Department of Mathematics, Faculty of Mathematics and Computer Science, Babeş-Bolyai University, Cluj-Napoca, Romania

Alin V. Roşca
Department of Statistics-Forecasts-Mathematics, Faculty of Economics and Business Administration, Babeş-Bolyai University, Cluj-Napoca, Romania, and

Ioan Pop
Department of Mathematics, Faculty of Mathematics and Computer Science, Babeş-Bolyai University, Cluj-Napoca, Romania

Abstract

Purpose – This study aims to study the mixed convection flow and heat transfer of Al_2O_3-Cu/water hybrid nanofluid over a vertical plate. Governing equations for conservation of mass, momentum and energy for the hybrid nanofluid over a vertical flat plate are introduced.

Design/methodology/approach – The similarity transformation approach is used to transform the set of partial differential equations into a set of non-dimensional ordinary differential equations. Finite-deference with collocation method is used to integrate the governing equations for the velocity and temperature profiles.

Findings – The results show that dual solutions exist for the case of opposing flow over the plate. Linear stability analysis was performed to identify a stable solution. The stability analysis shows that the lower branch of the solution is always unstable, while the upper branch of the solution is always stable. The results of boundary layer analysis are reported for the various volume fractions of composite nanoparticles and mixed convection parameter. The outcomes show that the composition of nanoparticles can notably influence the boundary layer flow and heat transfer profiles. It is also found that the trend of the variation of surface skin friction and heat transfer for each of the dual solution branches can be different. The critical values of the mixed convection parameter, λ, where the dual solution branches joint together, are also under the

This work of Mohammad Ghalambaz was supported by the STAR Institute – UBB, Cluj-Napoca, Romania, External Fellowship program, and the work by Natalia C. Roşca, Alin V. Roşca and Ioan Pop has been supported from the Grant PN-III-P4-ID-PCE-2016-0036, UEFISCDI, Romanian Ministry of Sciences. The authors thank the very competent reviewers for their constructive comments, which clearly improved the quality of the manuscript.

International Journal of Numerical Methods for Heat & Fluid Flow
Vol. 30 No. 7, 2020
pp. 3737-3754

0961-5539
DOI 10.1108/HFF-08-2019-0661

influence of the composition of hybrid nanoparticles. For instance, assuming a total volume fraction of 5 per cent for the mixture of Al_2O_3 and Cu nanoparticles, the critical value of mixing parameter of λ changes from -3.1940 to -3.2561 by changing the composition of nanofluids from Al_2O_3 (5 per cent) + Cu (0%) to Al_2O_3 (2.5%) + Cu (2.5 per cent).

Originality/value – The mixed convection stability analysis and heat transfer study of hybrid nanofluids for a stagnation-point boundary layer flow are addressed for the first time. The introduced hybrid nanofluid model and similarity solution are new and of interest in both mathematical and physical points of view.

Keywords Stability analysis, Dual solutions, Heat transfer enhancement, Numerical method, Hybrid nanofluids, Mixed convection flow

Paper type Research paper

1. Introduction

Convective flows have been subject of great attention to scientists from both practical and theoretical points of view. Such attention is because of the vast occurrence of convective flows in various engineering and geophysical fields, including, geothermal energy extraction, nuclear waste disposal, groundwater movement, thermal insulation, solid-matrix heat-exchangers, drying porous solids oil and gas production and many others. Mixed convection heat transfer, where induced because of the interaction between an internally generated buoyancy forces and an imposed flow, are also substantial in crystal growth, solar collectors, nuclear reactors and cooling of electronic systems Lok *et al.* (2017).

Stagnation-point flows, which are referred to flows about the front of a blunt-nosed body or the stagnation region, occur on bodies moving in a fluid. The stagnation region encounters the highest rates of mass deposition, the highest heat transfer and the highest pressure. Hiemenz (1911) was the first researcher who used a similarity transform to addressed the two-dimensional stagnation-point flows by reducing the partial differential Navier–Stokes equations to a set of nonlinear ordinary differential equations. Homann (1936) later solved the axisymmetric case of stagnation-point flows. In the past several years, extensive attention has been attracted to various aspects of the stagnation-point flows such as forced, free and mixed convection of a viscous fluid. The stagnation-point flows have been discussed in excellent published books by Schlichting and Gersten (2000), Gebhart *et al.* (1988), White and Corfield (2006) and Pop and Ingham (2001) and in the papers by Roşca and Pop (2013b) and Ramachandran *et al.* (1988).

In the past several years, much interest has been attracted to the synthesis of various types of nanofluids. Nanoparticles are miniature particles with at least one dimension in nanoscale size. The research on synthesis and study of nanoparticle properties is the subject of many scientific investigations because of numerous substantial practices in electronic, optical and biomedical fields. The nanofluids which are a stable suspension of a base liquid and nanoparticles were first introduced by Choi (1995) in 1995. Later, Khanafer *et al.* (2003) addressed the thermal advantage of using nanofluids in an enclosure. After that, many researchers argued the models and advantages of using nanoparticles for different base fluids and practical applications. Various applications of nanofluids are well established in books by Minkowycz *et al.* (2013), Nield and Bejan (2017), Das *et al.* (2007) and Shenoy *et al.* (2016), and in the reviews by Wong and De Leon (2011), Kakaç and Pramuanjaroenkij (2009), Buongiorno *et al.* (2009), Sheikholeslami and Ganji (2016), Mahian *et al.* (2013; 2018a, 2018b), Manca *et al.* (2010), Mahdi *et al.* (2015), Myers *et al.* (2017), Ahmadi *et al.* (2018) and Groşan *et al.* (2017). Heat transfer coefficients of prepared base and nanofluids were also measured by Ahmadi and Willing (2018) using a lab-built test rig.

After the study of Huminic and Huminic (2018), the hybrid nanofluids are synthesized by using two or more solid nanoparticles to obtain a stable suspension of composite nanoparticles

in classical fluids such as water, water ethylene glycol mixture, kerosene and engine oils. The hybrid nanofluids show enhanced thermophysical properties benefiting the advantage of two types of nanoparticles. The solid nanoparticles used for synthesizing of nanofluids are: Al_2O_3–Cu, Al_2O_3–Ag, Cu–Cu_2O, Cu–Zn, Ag–TiO_2, Ag–MnO, Ag–CNT, Al_2O_3–MEPCM, Cu–TiO_2 and Al_2O_3 – SiO_2. During the very recent years, the hybrid nanofluids have been subject of numerous engineering practices such as micro-channel, mini-channel heat sink, heat pipes, air-conditioning system and various types of heat exchangers included as shell and tube, plate, tubular, tube in tube coiled and helically coiled heat exchangers. Comprehensive reviews on hybrid nanofluids were presented by Sarkar *et al.* (2015), Akilu *et al.* (2016), Sidik *et al.* (2016), Sundar *et al.* (2017) and Babu *et al.* (2017). We also mention here the papers by Ghalambaz *et al.* (2019b, 2019a), Hayat *et al.* (2018), Devi and Devi (2016) and Tayebi and Chamkha (2017). However, Jana *et al.* (2007) in 2007 have published the first paper about the thermal conductivity of hybrid nanofluids. They synthesized and examined the thermal conductivity of nanofluids based on gold nanoparticles, copper and carbon nanotubes as well as hybrid nanofluids, including carbon nanotube–gold/water and carbon nanotube–copper/water. Various studies show that using a hybrid nanofluid can enhance the thermophysical properties of the suspension and improving the heat transfer.

The present study aims to theoretically study the mixed convection flow and heat transfer of hybrid nanofluids over a vertical plate. The mixed convection heat transfer over a vertical plate is a benchmark problem in many heat transfer applications. By the study of the boundary layer heat transfer of hybrid nanofluids over a vertical plate, the following fundamental questions will be addressed for the first time. How the presence of hybrid nanoparticles would affect the stability of the boundary layer for dual solutions? What is the heat transfer behavior of a hybrid nanofluid by changing the composition of nanofluid from a single type of nanoparticle to a hybrid composite particle? What is the effect of the presence of the secondary nanoparticles on each of the dual solutions?

2. Mathematical model

Consider a two-dimensional viscous steady-state boundary layer flow and heat transfer of a hybrid nanofluid over a flat plate with a linear temperature distribution as shown in Figure 1. The Cartesian coordinate system is illustrated in Figure 1. It is assumed that there is a non-uniform fluid flow over the plate with the velocity of $U_e(x)$ flowing along with the positive coordinate system in an upward direction. It is also assumed that the surface temperature is

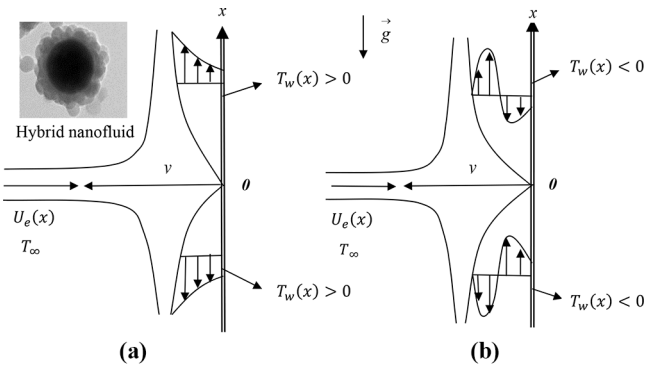

Notes: (a) Assisting flow; (b) opposing flow

Figure 1.
Physical model and coordinate system

$T_w(x)$ while the far-field fluid is at the constant temperature T_∞. The plate can be hot or cold which results in assessing or opposing mixed convection flows. The working fluid is a hybrid nanofluid consisting of two different types of nanoparticle composites, and the base fluid is water. The geometry of a simple flat plate is adopted in this research as a well-known benchmark problem for the study of external boundary layer flows. The hybrid nanofluid next to the hot surface tends to move upward because of the buoyancy force and inducing an assessing flow. However, when the surface is cold, the hybrid nanofluid tends to flow in a downward direction, resulting in an opposing flow natural convection flow. It is assumed that the size of nanoparticles is uniform, and the hybrid nanofluid is a stable suspension of composite nanoparticles, and hence, the agglomeration effects are neglected.

The governing equations of the conservations of the nanofluid mass, momentum and energy by uing the usual boundary layer approximation are written as (Roşca and Pop, 2013b; Roşca and Pop, 2013a; Weidman *et al.*, 2006):

$$\frac{\partial u}{\partial x}+\frac{\partial v}{\partial y}=0 \tag{1}$$

$$u\frac{\partial u}{\partial x}+v\frac{\partial u}{\partial y}=g\beta_{hnf}(T-T_\infty)+U_e\frac{dU_e}{dx}+\frac{\mu_{hnf}}{\rho_{hnf}}\frac{\partial^2 u}{\partial y^2} \tag{2}$$

$$u\frac{\partial T}{\partial x}+v\frac{\partial T}{\partial y}=\frac{k_{hnf}}{(\rho C_p)_{hnf}}\frac{\partial^2 T}{\partial y^2} \tag{3}$$

subject to:

$$\begin{aligned} &u=0, v=0, T=T_w(x)=T_\infty+T_0(x/L)\\ &u\to U_e(x), T\to T_\infty \quad \text{as} y\to\infty \end{aligned} \tag{4}$$

where L is the characteristic length of the plate. The ambient velocity is considered as $U_e(x) = a\ x$, where a is a positive constant. As seen in the boundary conditions, the temperature of the surface varies linearly as $T_w(x) - T_\infty \cong T_0 x/L$, where T_0 is a constant characteristic temperature. As the hybrid nanofluid flows in the positive direction, the scale temperature T_0 can be positive or negative. The positive values of T_0 correspond to the hot plate with assisting flows, and its negative values correspond to cold plate with opposing mixed convection flow. In the above governing equations, it is assumed that the Reynolds number is adequately large (Noghrehabadi *et al.*, 2014), and hence, the error because of the boundary layer assumptions is minimal.

Some equations for evaluating the thermophysical properties of hybrid nanofluids are required. The thermophysical properties of various nanoparticles and water as the base fluid are summarized in Table I. In the present study, Al_2O_3–Cu/water nanofluid is adopted. This nanofluid was studied by Ashorynejad and Shahriari (2018) for a case of natural convection in a cavity. The effective thermal diffusivity, effective density, dynamic viscosity, heat capacity, thermal conductivity and thermal volume coefficient of hybrid nanofluids can be evaluated using the relations introduced in Table II.

Now, using the following similarity variables, the governing partial differential equations can be converted into a non-dimensional form:

$$u=axf'(\eta), v=-\sqrt{a\nu_f}f(\eta), \theta(\eta)=\frac{T-T_\infty}{T_w-T_\infty}, \eta=y\sqrt{\frac{a}{\nu_f}} \tag{5}$$

where u and v denote the x and y components of velocity, respectively. Now, invoking the similarity variables (5), equations (2) and (3) along with the boundary conditions (4) are transformed into the following similarity ordinary differential equations:

$$\frac{\mu_{hnf}/\mu_f}{\rho_{hnf}/\rho_f} f''' + \frac{\beta_{hnf}}{\beta_f} \lambda\, \theta + f f'' + 1 - f'^2 = 0 \tag{6}$$

$$\frac{1}{Pr} \frac{k_{hnf}/k_f}{(\rho C_p)_{hnf}/(\rho C_p)_f} \theta'' + f\theta' - f'\theta = 0 \tag{7}$$

The corresponding boundary conditions at the plate surface and the asymptotic boundary conditions are:

$$\begin{aligned} &f(0) = 0, f'(0) = 0, \theta(0) = 1 \\ &f'(\eta) \to 1, \theta(\eta) \to 0 \text{ as } \eta \to \infty \end{aligned} \tag{8}$$

Properties	Cu	Al_2O_3	Basefluid (water)
ρ (kg/m^3)	8,933	3,970	997.1
Cp (J/kg.K)	385	765	4179.0
k (W/m.K)	400	40	0.613
$\alpha \times 10^7$	1,163.1	131.7	1.47
β (1/K) $\times 10^6$	50.1*	25.5*	210
Nanoparticles size (nm)	20	–	–

Note: *The linear thermal expansion coefficient is multiplied by three to obtain the volumetric thermal expansion

Sources: Hayat *et al.* (2018); Devi and Devi, (2016); Tayebi and Chamkha (2017); Ashorynejad and Shahriari (2018); Kamyar *et al.* (2012)

Table I. The thermophysical properties of the base fluid and nanoparticles

Properties	*Nanofluids*	*Hybrid nanofluids*
Density	$\rho_{nf} = (1-\phi)\rho_f + \phi\rho_s$	$\rho_{hnf} = \phi_1\rho_{s1} + \phi_2\rho_{s2} + (1-\phi_{hnf})\rho_f$
Heat capacity	$(\rho C_p)_{nf} = (1-\phi)(\rho C_p)_f + \phi(\rho C_p)_s$	$(\rho C_p)_{hnf} = \phi_1(\rho C_p)_{s1} + \phi_2(\rho C_p)_{s2} + (1-\phi_{hnf})(\rho C_p)_f$
Dynamic viscosity	$\frac{\mu_{nf}}{\mu_f} = \frac{1}{(1-\phi)^{2.5}}$	$\frac{\mu_{hnf}}{\mu_f} = \frac{1}{(1-\phi_1-\phi_2)^{2.5}}$
Thermal conductivity	$\frac{k_{nf}}{k_f} = \frac{k_s + 2k_f - 2\phi(k_f - k_s)}{k_s + 2k_f + 2\phi(k_f - k_s)}$	$\frac{k_{hnf}}{k_f} = \left[\frac{\frac{(\phi_1 k_1 + \phi_2 k_2)}{\phi_{hnf}} + 2k_f + 2(\phi_1 k_1 + \phi_2 k_2) - 2\phi_{hnf} k_f}{\frac{(\phi_1 k_1 + \phi_2 k_2)}{\phi_{hnf}} + 2k_f - 2(\phi_1 k_1 + \phi_2 k_2) - 2\phi_{hnf} k_f}\right]$
Thermal expansion	$(\rho\beta)_{nf} = (1-\phi)(\rho\beta)_f \phi(\rho\beta)_s$	$\beta_{hnf} = \phi_1\beta_{s1} + \phi_2\beta_{s2} + (1-\phi_{hnf})\beta_f$ where $\phi_{hnf} = \phi_1 + \phi_2$

Source: Babu *et al.* (2017)

Table II. Thermal properties of nanofluids and hybrid nanofluids

In the above equations, primes show the differentiation with respect to independent variable of η. Here, λ is the constant parameter for mixed convection, which is defined as:

$$\lambda = \frac{Gr_x}{Re_x^2} \tag{9}$$

with $Gr_x = g\beta_f(T_w - T_\infty)x^3/\nu_f^2$ being the local Grashof number and $Re_x = U_e(x)\,x/\nu_f$ is the local Reynolds number; so that $\lambda = g\,\beta_f T_0/a^2$. It should be noted that $\lambda > 0$ corresponds to assisting flow, $\lambda = -0$ is for forced convection flow and $\lambda < 0$ corresponds to opposing flow.

It is worth mentioning that when $\phi_1 = \phi_2 = 0$, equations (6) and (7) reduce to:

$$f''' + \lambda\,\theta + ff'' + 1 - f'^2 = 0 \tag{10}$$

$$\frac{1}{Pr}\theta'' + f\theta' - f'\theta = 0 \tag{11}$$

subject to the boundary conditions (8). These equations are similar to equations (17) and (18) from Ramachandran *et al.* (1988) when $n = 1$.

The skin friction coefficient C_f and the local Nusselt number are the physical quantities of interest. The skin friction coefficient and local Nusselt number are introduced as:

$$C_f = \frac{\tau_w}{\frac{1}{2}\rho_f U_e(x)^2}, Nu_x = -k_{hnf}\left(\frac{\partial T}{\partial y}\right)_{y=0} \tag{12}$$

where τ_w denotes shear stress or the skin friction along with the plate, and q_w denotes the surface heat flux. Shear stress and surface heat flux are defined by:

$$\tau_w = \mu_{hnf}\left(\frac{\partial u}{\partial y}\right)_{y=0}, \quad q_w = -k_{hnf}\left(\frac{\partial T}{\partial y}\right)_{y=0} \tag{13}$$

Using equations (5), (12) and (13), we get:

$$\frac{1}{2}Re_x^{1/2}C_f = \frac{\mu_{hnf}}{\mu_f}f''(0), Nur = Re_x^{-1/2}Nu_x = -\frac{k_{hnf}}{k_f}\theta'(0) \tag{14}$$

where $Re_x = U_e(x)x/\nu_f$ is the local Reynolds number.

3. Flow stability

There are two solutions for the boundary value problem [equations (6)-(8)], which are the stable and unstable solutions. These solutions can be identified by performing a stability analysis. The stability analysis was performed following Weidman *et al.* (2006) and the studies of Roşca and Pop (2013b, 2013a) by introducing a new time variable $\tau = a\,t$ in a non-dimensional form. The implication of τ constructs an initial value problem. This initial value problem is consistent with the solutions of boundary value problem. We have now:

$$u = axf'(\eta,\tau) v = -\sqrt{a\nu_f} f(\eta,\tau), \theta(\eta,\tau) = \frac{T - T_\infty}{T_w - T_\infty},$$
$$\eta = y\sqrt{\frac{a}{\nu_f}}, \tau = at \tag{15}$$

Thus, equations (6) and (7) can be written as:

$$\frac{\mu_{hnf}/\mu_f}{\rho_{hnf}/\rho_f}\frac{\partial^3 f}{\partial \eta^3} + \frac{\beta_{hnf}}{\beta_f}\lambda\,\theta + f\frac{\partial^2 f}{\partial \eta^2} + 1 - \left(\frac{\partial f}{\partial \eta}\right)^2 - \frac{\partial^2 f}{\partial \eta \partial \tau} = 0 \tag{16}$$

$$\frac{1}{Pr}\frac{k_{hnf}/k_f}{(\rho C_p)_{hnf}/(\rho C_p)_f}\frac{\partial^2 \theta}{\partial \eta^2} + f\frac{\partial \theta}{\partial \eta} - \frac{\partial f}{\partial \eta}\theta - \frac{\partial \theta}{\partial \tau} = 0 \tag{17}$$

The transformed boundary conditions at the surface and the asymptotic boundary conditions are:

$$f(0,\tau) = 0, f'(0,\tau) = 0, \theta(0,\tau) = 1$$
$$f'(\eta,\tau) \to 1, \theta(\eta,\tau) \to 0 \text{ as } \eta \to \infty \tag{18}$$

The stability analysis of the steady-state flow solution was examined by setting $f(\eta) = f_0(\eta)$ and $\theta(\eta) = \theta_0(\eta)$ in a way that the zero solutions satisfy the initial boundary-value introduced in equations (6)-(8). Hence, we can write $f(\eta, \tau)$ as (Weidman *et al.*, 2006):

$$f(\eta,\tau) = f_0(\eta) + e^{-\gamma\tau}F(\eta,\tau), \theta(\eta,\tau) = \theta_0(\eta) + e^{-\gamma\tau}G(\eta,\tau) \tag{19}$$

where $F(\eta, \tau)$ and $G(\eta, \tau)$ are minor compared to $f_0(\eta)$ and $\theta_0(\eta)$ in the above equation. Here, the unknown eigenvalue parameter is denoted by γ. Invoking equation (19), (16) and (17) become:

$$\frac{\mu_{hnf}/\mu_f}{\rho_{hnf}/\rho_f}\frac{\partial^3 F}{\partial \eta^3} + \frac{\beta_{hnf}}{\beta_f}\lambda G + f_0\frac{\partial^2 F}{\partial \eta^2} - \left(2f_0' - \gamma\right)\frac{\partial F}{\partial \eta} + f_0'' F - \frac{\partial^2 F}{\partial \eta \partial \tau} = 0 \tag{20}$$

$$\frac{1}{Pr}\frac{k_{hnf}/k_f}{(\rho C_p)_{hnf}/(\rho C_p)_f}\frac{\partial^2 G}{\partial \eta^2} + f_0\frac{\partial G}{\partial \eta} - \left(f_0' - \gamma\right)G + F\theta_0' - \frac{\partial F}{\partial \eta}\theta_0 - \frac{\partial G}{\partial \tau} = 0 \tag{21}$$

The corresponding boundary conditions are:

$$F(0,\tau) = 0, \frac{\partial F}{\partial \eta}(0,\tau) = 0, G(0,\tau) = 0$$
$$\frac{\partial F}{\partial \eta}(\eta,\tau) \to 0, G(\eta,\tau) \to 0 \text{ as } \eta \to \infty \tag{22}$$

The steady boundary layer solutions for $f_0(\eta)$ and $\theta_0(\eta)$ has to be investigated. This is done by setting $\tau = 0$, and as a result, an initial growth or decay of the solution equation (19) could be verified by $F = F_0(\eta)$ and $G = G_0(\eta)$ in equations (20) and (21).

$$\frac{\mu_{hnf}/\mu_f}{\rho_{hnf}/\rho_f}F_0''' + \frac{\beta_{hnf}}{\beta_f}\lambda G_0 + f_0 F_0'' - \left(2f_0' - \gamma\right)F_0' + f_0'' F_0 = 0 \tag{23}$$

$$\frac{1}{Pr}\frac{k_{hnf}/k_f}{(\rho C_p)_{hnf}/(\rho C_p)_f}G_0'' + f_0 G_0' - \left(f_0' - \gamma\right)G_0 + F_0\theta_0' - F_0'\theta_0 = 0 \tag{24}$$

along with the boundary conditions:

$$\begin{aligned} &F_0(0) = 0, F_0'(0) = 0, G_0(0) = 0 \\ &F_0'(\eta) \to 0, G_0(\eta) \to 0 \text{ as } \eta \to \infty \end{aligned} \tag{25}$$

For particular values of Pr and λ, the stability of the corresponding steady flow problem equations (6)-(8) is determined by calculating the smallest eigenvalue of the equations. Following Harris *et al.* (2009), a boundary condition on $F_0(\eta)$ or $G_0(\eta)$ can be relaxed to seek the feasible eigenvalues of the equations. Therefore, here the condition that $F_0'(\eta) \to 0$ as $\eta \to \infty$ is relaxed. Then the system of equations (6) and (7) along with $F_0''(0) = 1$ as the new boundary condition is solved for a fixed value of γ.

4. Numerical method and code validation

Following Shampine *et al.* (2000), a finite-difference solver is used to numerically integrate the system of equations (6) and (7) along with the boundary conditions equation (8). The finite difference solver uses a collocation method with automatic grid adaptation to control the error and convergence of the solution. As the governing equations are solved in a large domain with an asymptotic boundary condition, the gradients near the surface are high while they are almost zero at the asymptotic condition. Hence, a dense grid is required next to the surface, while a coarse grid is adequate for far-field. Thus, the grid adaptation is used to control the computational cost and accuracy. The Newton method is used as the iteration method for with a maximum relative error of 10^{-9} as the convergence limit. The stability equations are based on the boundary layer equations. Hence, the numerical solution of equations (6) and (7) were incorporated as a known solution in the stability analysis of equations (23) and (24) subject to the boundary equation (25). The same finite difference approach was used to integrate differential equations (23) and (24).

One of the important aspects of the present study was choosing an adequate value of η_∞. The value of η_∞ should be large enough to capture the asymptotic behavior of the solution. Thus, the solution process was initiated with an initial value of $\eta_\infty = 5$ and then equations (6) and (7) were solved. Then the value of η_∞ was increased, and $\theta'(0)$, as well as $f''(0)$, were monitored until the increment of η_∞ does not induce changes in the $\theta'(0)$ and $f''(0)$. By performing numerical experiments, it was found that $\eta_\infty = 10$ can satisfy the asymptotic boundary condition for the range of studied non-dimensional parameters. Another important point of the present numerical solution is the existence of a dual solution. To capture dual solutions, a continuation approach by starting adequate initial guesses was used.

To check the accuracy of the solution, the obtained values of $\theta'(0)$ and $f''(0)$ are compared with the results of Ramachandran *et al.* (1988) when $\phi = 0$. The results are summarized in Figure 2 and Table III. These tables confirm that there is a very good agreement between the literature results and the outcomes of the present work.

5. Results and discussion

In the present study, Al_2O_3-Cu/water nanofluid is adopted as the hybrid nanofluid. This nanofluid was experimentally used in (Suresh *et al.*, 2012). In the first part of the present study, the stability analysis of the two branches of the solution was addressed.

5.1 Stability analysis

Now the linear equations (23) and (24) subject to the homogeneous boundary conditions equation (25) constitutes an eigenvalue problem, in which the eigenvalue is γ. This eigenvalue problem has infinite number of eigenvalues $\gamma_1 < \gamma_2 < \gamma_3 < \ldots < \gamma_n < \ldots$. if the negative smallest value of γ_1 indicates that disturbances can grow in the flow and then the flow is unstable. However, a positive value of γ_1 indicates that the disturbances would

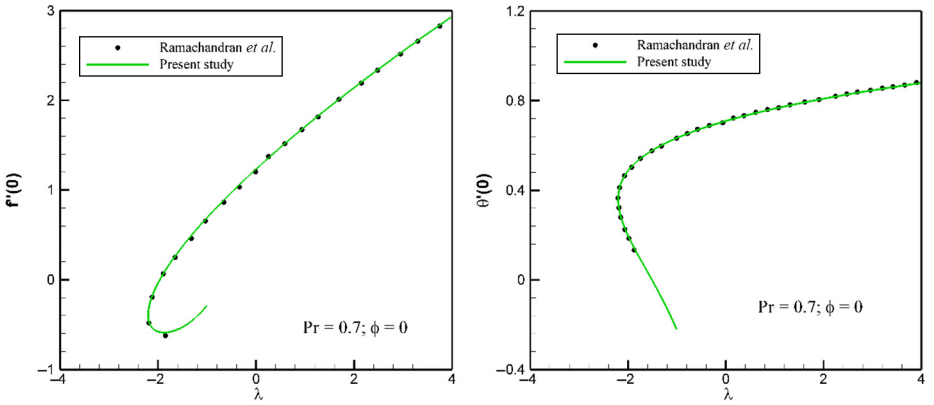

Figure 2. A comparison between the present outcomes and the outcomes reported by Ramachandran *et al.* (1988) in the case of pure flow $\phi = 0$

Table III. A comparison between the present outcomes and those reported by Ramachandran *et al.* (1988) in the case of pure flow $\phi = 0$

	$\lambda = 1$				$\lambda = -1$			
	Ramachandran *et al.* (1988)		Present study		Ramachandran *et al.* (1988)		Present study	
Pr	$f''(0)$	$-\theta'(0)$	$f''(0)$	$-\theta'(0)$	$f''(0)$	$-\theta'(0)$	$f''(0)$	$-\theta'(0)$
0.7	1.7063	0.7641	1.7063	0.7641	0.6917	0.6332	0.6917	0.6332
7.0	1.5179	−1.7224	1.5179	−1.7224	0.9235	1.5460	0.9235	1.5460
20	1.4485	2.4576	1.4485	2.4576	1.0031	2.2683	1.0031	2.2683

Table IV. Smallest eigenvalues γ for various values of $\lambda < 0$, the case of opposing flow, when the Al_2O_3 nanoparticles are within a fixed volume fraction as $\phi_1 = 0.05$

ϕ_1 Al_2O_3	ϕ_2 Cu	λ	Upper branch γ	Lower branch γ
0.05	0	−2	1.0392	−0.8907
		−2.5	0.8085	−0.7196
		−3.3	0.1507	−0.1475
0.05	0.025	−2	1.0155	−0.8687
		−2.5	0.7373	−0.6605
		−3	0.2999	−0.2870
0.05	0.05	−2	0.9797	−0.8398
		−2.5	0.6448	−0.5843
		−2.9	0.1236	−0.1213

decay in the fluid and then the flow is stable. Here, as we only study the smallest value of γ_1, the eigenvalue γ indicates γ_1. Tables IV and V show the smallest eigenvalue of each solution branch for different compositions of hybrid nanoparticles. As seen, regardless of the composition of hybrid nanoparticles, all of the lower solution branches are unstable with negative values of the smallest eigenvalue.

5.2. Flow and heat transfer analysis

In the following, the total volume fraction of hybrid nanoparticles is adapted to be constant as $\phi_{hnf} = 0.05$, but the combination of each type of nanoparticles can be changed. Besides, the results were also studied for cases with 5 per cent volume fraction of one nanoparticle and the change of the volume fraction of another nanoparticle in the range of 0-5 per cent volume fraction.

Figures 3 and 4 depict the velocity and temperature profiles of the hybrid nanofluid, respectively. The results are plotted for the case of the opposing convection with $\lambda = -2.5$. In this case, there is a dual solution for flow and heat transfer over the plate. Both solutions are captured and plotted in these figures. The effect of the variation of the combination of composite volume fraction is studied in these figures. The velocity profiles in the lower solution branch indicate the effect of opposing flow by changing the velocity direction in the vicinity of the plate.

The upper solution branch is slightly under the influence of the opposing flow and almost linearly changes next to the hot plate. Both of the lower and upper branches of the boundary

Table V. Smallest eigenvalues γ for various values of opposing flow ($\lambda < 0$) when the Cu nanoparticles are at a fixed volume fraction of $\phi_2 = 0.05$

ϕ_1 Al_2O_3	ϕ_2 Cu	λ	Upper branch γ	Lower branch γ
0	0.05	−2	1.0411	−0.8867
		−2.5	0.7792	−0.6935
		−3.1	0.2771	−0.2660
0.025	0.05	−2	1.0134	−0.8653
		−2.5	0.7187	−0.6447
		−3	0.2120	−0.2054
0.05	0.05	−2	0.9797	−0.8398
		−2.5	0.6448	−0.5843
		−2.9	0.1236	−0.1213

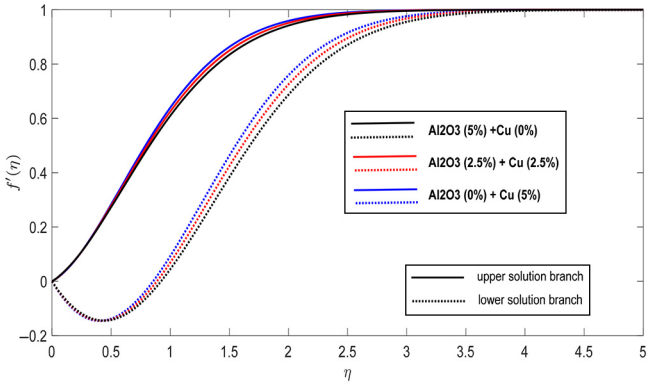

Figure 3. Velocity profiles for the hybrid nanofluid when the total volume fraction of hybrid nanoparticles is constant as $\phi_{hnf} = 0.05$ and $\lambda = -2.5$

layer velocities approach to the asymptotic value of unity when η tends to large values. The thickness of the boundary layer in the case of the lower solution branch is much higher than that of the upper solution branch. Figure 4 shows the corresponding temperature profiles for the lower and upper solution branches. As seen, the thermal boundary layer thickness of the upper solution branch is smaller than that of the lower solution branch.

Consequently, it can be observed that the temperature gradient next to the plate, i.e. $\eta = 0$, in the case of the upper solution branch is higher than that of the lower solution branch. This is because of the influence of velocity profiles. In the case of the upper solution branch, the velocity gradient and slope of the velocity profiles, next to the wall is considerably higher than that of the lower solution branch.

Attention to the effect of the volume concentration of nanoparticles composites depicts that the change of the composition from the pure Al_2O_3 to pure Cu nanoparticles mostly affect the flow of the lower branch solution. The most evident influence is in the middle of the boundary layer about $\eta = 2$. In these figures, the total concentration of composite nanoparticles is fixed at 5 per cent. The increase of the volume fraction of Cu nanoparticles (the decrease of Al_2O_3 volume fraction) increases the magnitude of the velocities and decreases the temperature in the boundary layer for both solutions. The effect of variation of the nanoparticle composition of the temperature profiles of the upper branch of the solution is almost negligible.

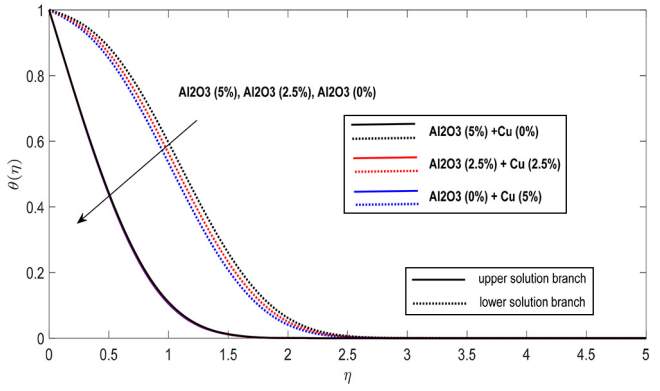

Figure 4. Temperature profiles for the hybrid nanofluid when the total volume fraction of hybrid nanoparticles is constant as $\phi_{hnf} = 0.05$ and $\lambda = -2.5$

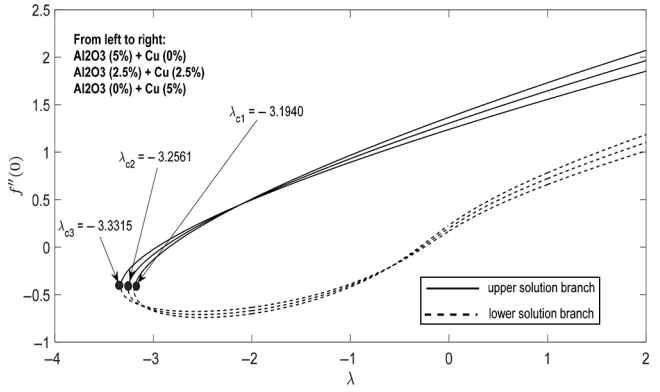

Figure 5. Variation of $f''(0)$ as a function of λ for the hybrid nanofluid when the total volume fraction of hybrid nanoparticles is constant as $\phi_{hnf} = 0.05$

Figures 5 and 6 illustrate the variation of $f''(0)$ and $-\theta'(0)$, respectively. These figures are plotted for the various compositions of nanoparticles and a total volume fraction of 5 per cent. The results are depicted as a function of λ in the range of -4 to $+2$. As mentioned the case of negative values of λ corresponds to opposing convection flows. The trend of the

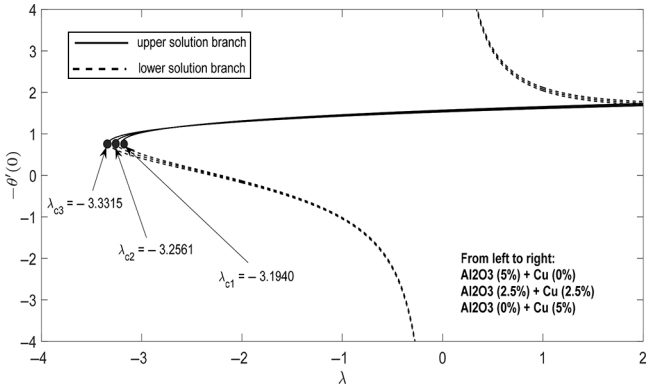

Figure 6.
Variation of $-\theta'(0)$ as a function of λ for the hybrid nanofluid when the total volume fraction of hybrid nanoparticles is constant as $\phi_{hnf} = 0.05$

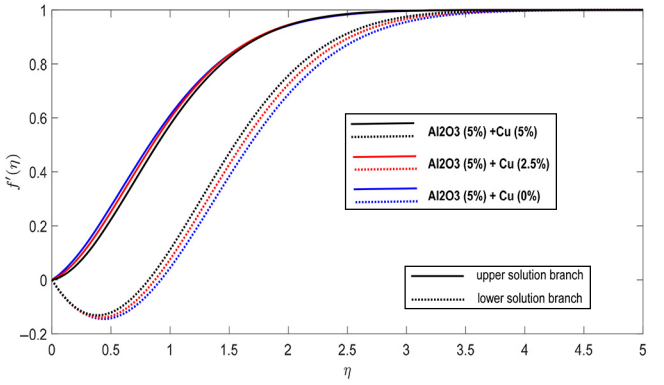

Figure 7.
Velocity profiles for the hybrid nanofluid when the volume fraction of Al_2O_3 nanoparticles is constant as $\phi_{nf} = 0.05$ and $\lambda = -2.5$

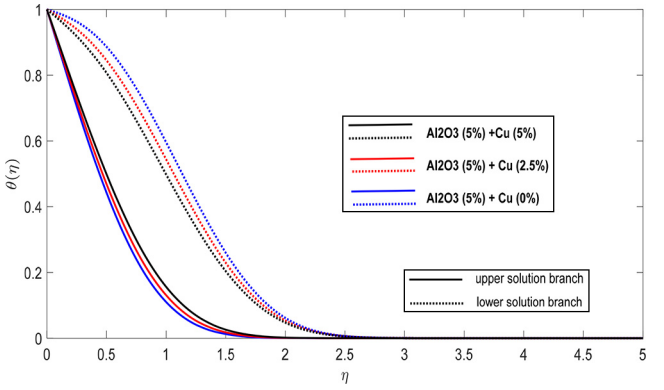

Figure 8.
Temperature profiles for hybrid nanofluid when the volume fraction of Al_2O_3 nanoparticles is constant as $\phi_{nf} = 0.05$ and $\lambda = -2.5$

behavior of the reduced skin friction, $f'(0)$, and the reduced temperature gradient, $\theta'(0)$, is a function of the variation of λ and the type of the solution branch. Considering the upper branch of the solution, the skin friction for a composite with a higher concentration of alumina is higher when λ is high, $\lambda > -2$. The same behavior is also true for the surface

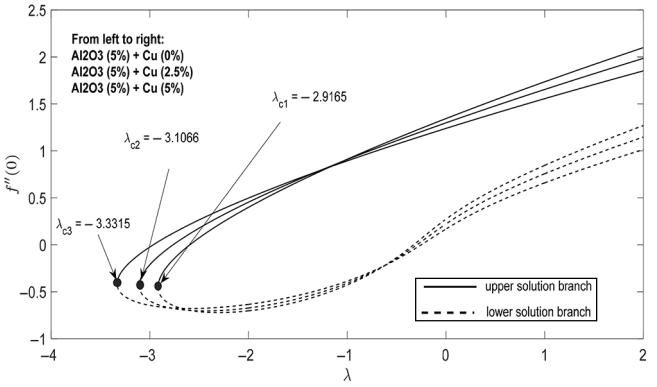

Figure 9.
Variation of $f''(0)$ as a function of λ for the hybrid nanofluid when the volume fraction of Al_2O_3 nanoparticles is constant as $\phi_{nf} = 0.05$

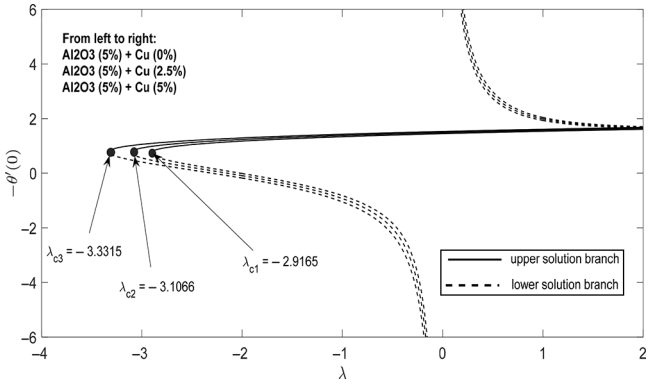

Figure 10.
Variation of $-\theta'(0)$ as a function of λ for the hybrid nanofluid when the volume fraction of Al_2O_3 nanoparticles is constant as $\phi_{nf} = 0.05$

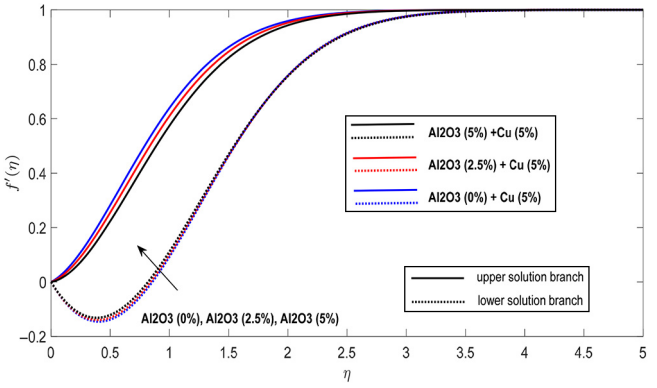

Figure 11.
Velocity profiles for the hybrid nanofluid when the volume fraction of Cu nanoparticles is constant as $\phi_{nf} = 0.05$ and $\lambda = -2.5$

temperature gradient. At a point about $\lambda = -2$ there is an inflection that changes the trend of the behavior of the surface skin friction and temperature gradient. The critical λ numbers which two branches of the solutions merge are $\lambda_{c1} = -3.1940$, $\lambda_{c2} = -3.2561$ and $\lambda_{c3} = -3.3315$ which corresponds to cases of Al_2O_3 (5 per cent) + Cu (0 per cent), Al_2O_3 (2.5 per

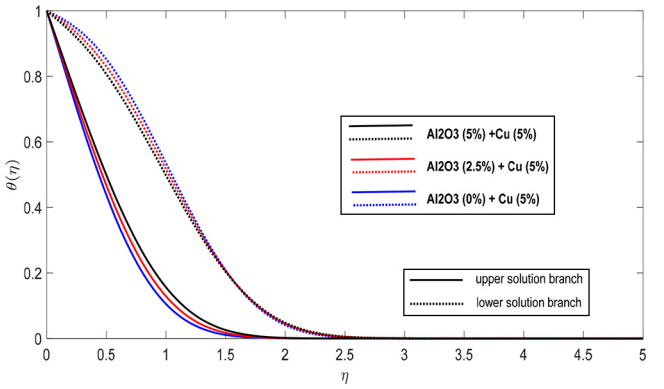

Figure 12.
Velocity profiles for the hybrid nanofluid when the volume fraction of Cu nanoparticles is constant as $\phi_{nf} = 0.05$ and $\lambda = -2.5$

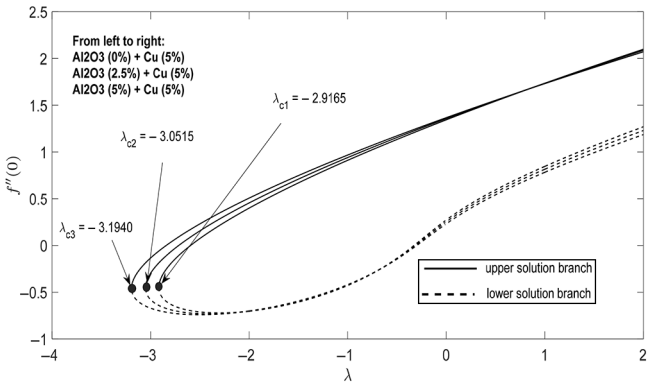

Figure 13.
Variation of $f'(0)$ as a function of λ for the hybrid nanofluid when the volume fraction of Cu nanoparticles is constant as $\phi_{nf} = 0.05$

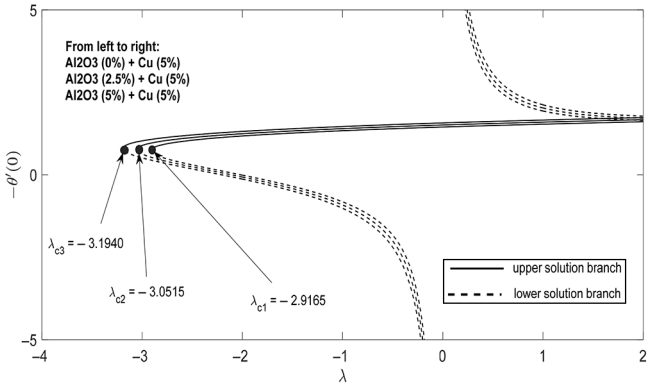

Figure 14.
Variation of $-\theta'(0)$ as a function of λ for the hybrid nanofluid when the volume fraction of Cu nanoparticles is constant as $\phi_{nf} = 0.05$

cent) + Cu (2.5 per cent) and Al_2O_3 (0 per cent) + Cu (5 per cent), respectively. By the increase of the concentration of copper nanoparticles the magnitude of critical λ number increases. In the case of critical λ, the magnitude of skin friction a temperature gradient for any composition of nanoparticles is the same.

Figures 7 and 8 respectively illustrate the velocity profiles and the temperature profiles for the hybrid nanofluid with a fixed volume fraction of 5 per cent Al_2O_3 nanoparticles and various volume fractions of Cu nanoparticles when $\lambda = -2.5$. Accordingly, Figures 9 and 10 depict $f''(0)$ and $-\theta'(0)$ as a function of λ. These figures show that the increase of the concentration of Cu nanoparticles increases the magnitude of the velocity and decreases the magnitude of temperature in the boundary layer for the lower solution branch. In contrast, the increase of the volume concentration of Cu nanoparticles decreases the magnitude of velocity and increases the temperature for the upper solution branch. The increase of volume fraction of Cu nanoparticles increases the critical value of λ. The increase of volume fraction of nanoparticles smoothly decreases the surface temperature gradient. Although the increase of concentration of Cu nanoparticles decreases the magnitude of $-\theta'(0)$, the overall heat transfer will be enhanced as the heat transfer is equal to the combination of $k_{hnf}/k_f \times \theta'(0)$. An increase in the concentration of Cu nanoparticles eventually enhances the overall heat transfer.

Similarly, Figures 11-14 depict the effect of variation of Al_2O_3 nanoparticles when the concentration of Cu nanoparticles is fixed as 5 per cent. Figure 11 interestingly shows that the upper branch of the solution is under the significant influence of the variation of the volume fraction of Al_2O_3 nanoparticles, but the effect of the variation of the volume fraction of Al_2O_3 on the lower branch is very smooth. Moreover, the variation of the volume concentration of Al_2O_3 nanoparticles affects both of the lower and upper branches solutions almost equally. Figures 13 and 14 in agreement with the trend of results of Figures 9 and 10 depict that the raise of the concentration of Al_2O_3 nanoparticles elevates the magnitude of λ.

6. Conclusion

Hybrid nanofluids are a new type of engineered fluids, synthesized as a composite mixture of two types of nanoparticles. The boundary layer flow and heat transfer of Al_2O_3-Cu/water nanofluid over a flat plate were addressed for various combinations of composite nanoparticles. The results are reported for various values of mixed convection parameter, λ, including assisting and opposing flow convection. The results show that there is a dual solution in some opposing flow situations. Using stability analysis, stable and unstable solutions were identified. The main outcomes of this study can be summarized as follows:

- There is a dual solution for flow and heat transfer of hybrid nanofluid over the plate in most of the opposing flow situations. The skin friction and heat transfer behavior of the hybrid nanofluid for each solution branch is different. For instance, considering a fixed composite nanoparticle volume fraction of 5 per cent and mixing parameter $\lambda < -2$, the increase of volume fraction of Cu nanoparticles decreases the magnitude of surface skin friction and heat transfer for an upper branch of the solution. However, this trend of results can be the same or opposite for the lower branch solution depending on the magnitude of mixing parameter λ. One of the most important parameters which significantly affect the trend of flow and heat transfer of hybrid nanofluids is the mixing parameter of λ.

- Regardless of the concentration and type of nanoparticles, the lower solution branch is always unstable with a negative smallest eigenvalue, while the upper solution branch is always stable with a positive smallest eigenvalue.
- For a fixed concentration of 5 per cent volume fraction of nanoparticles, an addition of Cu nanoparticles would significantly influence the boundary layer flow and temperature profiles for both upper and lower solution branches. However, for a fixed 5 per cent volume fraction of Cu nanoparticle, the addition of Al_2O_3 nanoparticles only slightly affects the lower solution branch. Hence, it can be concluded that the trend of the results is under the significant influence of the branch of the solution.
- Changing the composition of hybrid nanofluid from Al_2O_3 to Cu increases the magnitude of the critical value of mixing parameter λ. For large values of mixing parameter λ, the surface temperature gradient is almost independent of the composition of nanoparticles.

References

Ahmadi, M.H., Mirlohi, A., Nazari, M.A. and Ghasempour, R. (2018), "A review of thermal conductivity of various nanofluids", *Journal of Molecular Liquids*, Vol. 265, pp. 181-188.

Ahmadi, M. and Willing, G. (2018), "Heat transfer measurment in water based nanofluids", *International Journal of Heat and Mass Transfer*, Vol. 118, pp. 40-47.

Akilu, S., Sharma, K., Baheta, A.T. and Mamat, R. (2016), "A review of thermophysical properties of water based composite nanofluids", *Renewable and Sustainable Energy Reviews*, Vol. 66, pp. 654-678.

Ashorynejad, H.R. and Shahriari, A. (2018), "MHD natural convection of hybrid nanofluid in an open wavy cavity", *Results in Physics*, Vol. 9, pp. 440-455.

Babu, J.R., Kumar, K.K. and Rao, S.S. (2017), "State-of-art review on hybrid nanofluids", *Renewable and Sustainable Energy Reviews*, Vol. 77, pp. 551-565.

Buongiorno, J., Venerus, D.C., Prabhat, N., Mckrell, T., Townsend, J., Christianson, R., Tolmachev, Y.V., Keblinski, P., Hu, L.-W. and Alvarado, J.L. (2009), "A benchmark study on the thermal conductivity of nanofluids", *Journal of Applied Physics*, Vol. 106 No. 9, -094312.

Choi, S.U.S. (1995), "S.U.S. Choi, enhancing thermal conductivity of fluids with nanoparticles", in: Siginer, DA. and Wang, HP. (Eds). *Developments and Applications of Non-Newtonian Flows, American Society of Mechanical Engineers, New York, NY*.

Das, S.K., Choi, S.U., Yu, W. and Pradeep, T. (2007), *Nanofluids: science and Technology*, John Wiley and Sons, Hoboken, New Jersey.

Devi, S.S.U. and Devi, S.A. (2016), "Numerical investigation of three-dimensional hybrid Cu–Al2O3/water nanofluid flow over a stretching sheet with effecting Lorentz force subject to newtonian heating", *Canadian Journal of Physics*, Vol. 94 No. 5, pp. 490-496.

Gebhart, B. Jaluria, Y. Mahajan, R.L. and Sammakia, B. (1988), "Buoyancy-induced flows and transport", CRC Press, USA.

Ghalambaz, M., Chamkha, A.J. and Wen, D. (2019a), "Natural convective flow and heat transfer of nano-encapsulated phase change materials (NEPCMs) in a cavity", *International Journal of Heat and Mass Transfer*, Vol. 138, pp. 738-749.

Ghalambaz, M., Sheremet, M.A., Mehryan, S., Kashkooli, F.M. and Pop, I. (2019b), "Local thermal non-equilibrium analysis of conjugate free convection within a porous enclosure occupied with Ag–MgO hybrid nanofluid", *Journal of Thermal Analysis and Calorimetry*, Vol. 135 No. 2, pp. 1381-1398.

Groşan, T., Sheremet, M.A. and Pop, I. (2017), "Heat transfer enhancement in cavities filled with nanofluids", *Advances in New Heat Transfer Fluids*, CRC Press.

Harris, S., Ingham, D. and Pop, I. (2009), "Mixed convection boundary-layer flow near the stagnation point on a vertical surface in a porous medium: Brinkman model with slip", *Transport in Porous Media*, Vol. 77 No. 2, pp. 267-285.

Hayat, T., Nadeem, S. and Khan, A. (2018), "Rotating flow of Ag-CuO/H 2 O hybrid nanofluid with radiation and partial slip boundary effects", *The European Physical Journal E*, Vol. 41 No. 6, p. 75.

Hiemenz, K. (1911), "Die grenzschicht an einem in den gleichformigen flussigkeitsstrom eingetauchten geraden kreiszylinder", *Dinglers Polytech. J*, Vol. 326, pp. 407-410. 321-324,344-348,357-362,372-376,391-393.

Homann, F. (1936), "Der einfluss grosser zähigkeit bei der strömung um den zylinder und um die kugel", *ZAMM - Zeitschrift Für Angewandte Mathematik Und Mechanik*, Vol. 16 No. 3, pp. 153-164.

Huminic, G. and Huminic, A. (2018), "Hybrid nanofluids for heat transfer applications–a state-of-the-art review", *International Journal of Heat and Mass Transfer*, Vol. 125, pp. 82-103.

Jana, S., Salehi-Khojin, A. and Zhong, W.-H. (2007), "Enhancement of fluid thermal conductivity by the addition of single and hybrid nano-additives", *Thermochimica Acta*, Vol. 462 Nos 1/2, pp. 45-55.

Kakaç, S. and Pramuanjaroenkij, A. (2009), "Review of convective heat transfer enhancement with nanofluids", *International Journal of Heat and Mass Transfer*, Vol. 52 Nos 13/14, pp. 3187-3196.

Kamyar, A., Saidur, R. and Hasanuzzaman, M. (2012), "Application of computational fluid dynamics (CFD) for nanofluids", *International Journal of Heat and Mass Transfer*, Vol. 55 Nos 15/16, pp. 4104-4115.

Khanafer, K., Vafai, K. and Lightstone, M. (2003), "Buoyancy-driven heat transfer enhancement in a two-dimensional enclosure utilizing nanofluids", *International Journal of Heat and Mass Transfer*, Vol. 46 No. 19, pp. 3639-3653.

Lok, Y., Merkin, J. and Pop, I. (2017), "Mixed convection non-axisymmetric Homann stagnation-point flow", *Journal of Fluid Mechanics*, Vol. 812, pp. 418-434.

Mahdi, R.A., Mohammed, H., Munisamy, K. and Saeid, N. (2015), "Review of convection heat transfer and fluid flow in porous media with nanofluid", *Renewable and Sustainable Energy Reviews*, Vol. 41, pp. 715-734.

Mahian, O., Kianifar, A., Kalogirou, S.A., Pop, I. and Wongwises, S. (2013), "A review of the applications of nanofluids in solar energy", *International Journal of Heat and Mass Transfer*, Vol. 57 No. 2, pp. 582-594.

Mahian, O., Kolsi, L., Amani, M., Estellé, P., Ahmadi, G., Kleinstreuer, C., Marshall, J.S., Siavashi, M., Taylor, R.A. and Niazmand, H. (2018a), "Recent advances in modeling and simulation of nanofluid flows-part I: fundamental and theory", *Physics Reports*, Vol. 790, pp. 1-48.

Mahian, O., Kolsi, L., Amani, M., Estellé, P., Ahmadi, G., Kleinstreuer, C., Marshall, J.S., Taylor, R.A., Abu-Nada, E. and Rashidi, S. (2018b), "Recent advances in modeling and simulation of nanofluid flows-part II: applications", *Physics Reports*, Vol. 791, pp. 1-59.

Manca, O., Jaluria, Y. and Poulikakos, D. (2010), *Heat Transfer in Nanofluids*, Sage Publications Sage, London, England.

Minkowycz, W., Sparrow, E. and Abraham, J.P. (2013), *Nanoparticle Heat Transfer and Fluid Flow*, CRC press.

Myers, T.G., Ribera, H. and Cregan, V. (2017), "Does mathematics contribute to the nanofluid debate?", *International Journal of Heat and Mass Transfer*, Vol. 111, pp. 279-288.

Nield, D.A. and Bejan, A. (2017), *Convection in Porous Media*, 5th edition, Springer, New York.

Noghrehabadi, A., Izadpanahi, E. and Ghalambaz, M. (2014), "Analyze of fluid flow and heat transfer of nanofluids over a stretching sheet near the extrusion slit", *Computers and Fluids*, Vol. 100, pp. 227-236.

Pop, I. and Ingham, D.B. (2001), *Convective Heat Transfer: mathematical and Computational Modelling of Viscous Fluids and Porous Media*, Elsevier, Pergamon, Amsterdam.

Ramachandran, N., Chen, T. and Armaly, B.F. (1988), "Mixed convection in stagnation flows adjacent to vertical surfaces", *Journal of Heat Transfer*, Vol. 110 No. 2, pp. 373-377.

Roşca, A.V. and Pop, I. (2013a), "Flow and heat transfer over a vertical permeable stretching/shrinking sheet with a second order slip", *International Journal of Heat and Mass Transfer*, Vol. 60, pp. 355-364.

Roşca, N.C. and Pop, I. (2013b), "Mixed convection stagnation point flow past a vertical flat plate with a second order slip: heat flux case", *International Journal of Heat and Mass Transfer*, Vol. 65, pp. 102-109.

Sarkar, J., Ghosh, P. and Adil, A. (2015), "A review on hybrid nanofluids: recent research, development and applications", *Renewable and Sustainable Energy Reviews*, Vol. 43, pp. 164-177.

Schlichting, H. and Gersten, K. (2000), *Boundary-Layer Theory*, Springer, New York, NY.

Shampine, L.F., Kierzenka, J. and Reichelt, M.W. (2000), "Solving boundary value problems for ordinary differential equations in MATLAB with bvp4c", *Tutorial Notes*, pp. 1-27.

Sheikholeslami, M. and Ganji, D. (2016), "Nanofluid convective heat transfer using semi analytical and numerical approaches: a review", *Journal of the Taiwan Institute of Chemical Engineers*, Vol. 65, pp. 43-77.

Shenoy, A., Sheremet, M. and Pop, I. (2016), *Convective Flow and Heat Transfer from Wavy Surfaces: viscous Fluids, Porous Media, and Nanofluids*, CRC Press.

Sidik, N.A.C., Adamu, I.M., Jamil, M.M., Kefayati, G., Mamat, R. and Najafi, G. (2016), "Recent progress on hybrid nanofluids in heat transfer applications: a comprehensive review", *International Communications in Heat and Mass Transfer*, Vol. 78, pp. 68-79.

Sundar, L.S., Sharma, K., Singh, M.K. and Sousa, A. (2017), "Hybrid nanofluids preparation, thermal properties, heat transfer and friction factor–a review", *Renewable and Sustainable Energy Reviews*, Vol. 68, pp. 185-198.

Suresh, S., Venkitaraj, K., Selvakumar, P. and Chandrasekar, M. (2012), "Effect of Al2O3–Cu/water hybrid nanofluid in heat transfer", *Experimental Thermal and Fluid Science*, Vol. 38, pp. 54-60.

Tayebi, T. and Chamkha, A.J. (2017), "Buoyancy-driven heat transfer enhancement in a sinusoidally heated enclosure utilizing hybrid nanofluid", *Computational Thermal Sciences: An International Journal*, Vol. 9 No. 5, pp. 405-421.

Weidman, P., Kubitschek, D. and Davis, A. (2006), "The effect of transpiration on self-similar boundary layer flow over moving surfaces", *International Journal of Engineering Science*, Vol. 44 Nos 11/12, pp. 730-737.

White, F.M. and Corfield, I. (2006), *Viscous Fluid Flow*, McGraw-Hill New York, NY.

Wong, K.V. and De Leon, O. (2011), *Applications of Nanofluids: current and Future. Nanotechnology and Energy*, Jenny Stanford Publishing, Taylor & Francis Group.

Corresponding author
Mohammad Ghalambaz can be contacted at: mohammad.ghalambaz@tdtu.edu.vn